Functional Response of NiTi Elements for Smart Micro-actuation Applications

C.A. Biffi, A. Nespoli, B. Previtali, E. Villa, and A. Tuissi

(Submitted October 11, 2013; in revised form January 15, 2014; published online February 20, 2014)

1. Introduction

Shape memory alloys (SMAs) are functional materials, able to be used as active elements for smart actuation, thanks to the SMA (Ref 1, 2). The solid phase transition from a low temperature phase (martensite) to high temperature stable one (austenite), and viceversa, allows mechanical work to be generated, when a load is applied, because of the different mechanical response of the two phases. This displacement, which is produced by such peculiar effect, can be used for a controlled motion of components in mechanical systems (Ref 3), having a temporal response in the order of few Hz. This is due to the heat conduction, necessary for the phase transition; for making faster the temporal performance of such SMA devices, the solution is the minimization of the dimensions of these elements, so that the temperature change is more favorable in a shorter time, because of a minor mass to be cooled (Ref 4). In fact, the heating usually does not appear as a great limitation, because higher intensities of the electrical pulses can reduce the heating time. On the contrary, the cooling time can be more difficult to be controlled, as just the convection, natural or forced depending on the situation, is able to influence the phase transition from austenite to martensite.

C.A. Biffi, A. Nespoli, E. Villa, and **A. Tuissi**, Institute for Energetics and Interphases, National Research Council (CNR), Corso Promessi Sposi, 29, Lecco, Italy; and **B. Previtali**, Department of Mechanical Engineering, Politecnico di Milano, Via La Masa, 1, Milan, Italy. Contact e-mail: carlo.biffi@ieni.cnr.it.

Moreover, the scale down of the dimensions can also allow to obtain high power to weight ratio as function of the actuator weight and hence for their capability of generating high mechanical performance in very limited spaces (Ref 5).

Consequently, the indication of miniaturization of these smart active elements for actuators influences strongly the panorama of the manufacturing processes, suitable for their fabrication (Ref 6). Laser micromachining appears to be one of the easiest and convenient choices, because this manufacturing technology offers several advantages: opportunity of machining complex shapes with high flexibility, important level of industrialization, high productivity, and repeatability (Ref 7, 8). On the contrary, the most serious drawback of such a process generally is the significant thermal affection, which can be associated to the material damage, because of the heat flow, being used for melting and vaporizing the material during its removal from the workpiece (Ref 9). As a matter of fact, the main implication is the generation of thermal damages (melted material, heat affected zone, oxides, cracks), able to change the performances of the SMA elements from the nominal behavior, associated to the properties of the base material, not laser affected (Ref 10, 11). The necessity of additional post-processing (chemical, electro-chemical) is so of great importance in order to obtain back the initial functional properties of the material (Ref 12-14).

As previously reported, the possibility of shaping complex geometry, with respect to the use of a wire, allows solving the problem of the shape setting. Otherwise, the effect of the grain orientation could become more relevant to be evaluated on the functional performances, mainly if the element geometry is not developed in the principal direction of the previous plastic deformation processes (i.e., snake-like configuration). Moreover, the effect of the stabilization of the functional response during cycling, coupled with the texturing effect, can be another aspect to be investigated, because not completely studied in the literature.

In this context, the present paper has been focalized on the functional characterization of 90 μm thick micro-elements in quasi-equiatomic NiTi SMA, which were fabricated from thin

tapes by means laser microcutting and post-processed using a chemical etching. The geometry, selected for this work, was the called snake-like configuration, generally adopted for elements able to produce relevant strokes under the loading of intermediate levels of force (Ref 14, 15). It has been demonstrated that in the mini-scale the snake-like arrangement should be a good alternative (Ref 16, 17) to common configurations for actuators, such as the wire and the helical spring ones.

Calorimetric analysis was first proposed for the identification of the characteristic temperatures, to be used for the following thermo-mechanical testing; strain recovery tests were done with different levels of applied load and five thermal cycles were proposed at each applied load for the evaluation of the evolution of the mechanical response. The effect of post-thermal treatment and grain orientation were also evaluated on the final performances of the proposed SMA active element for smart micro-actuation.

2. Experimental

In this paragraph, the methods adopted for the material preparation and for the micro-elements fabrication were described. The definition of the geometry of the micro-elements as well as the types of characterization adopted in this work were also reported.

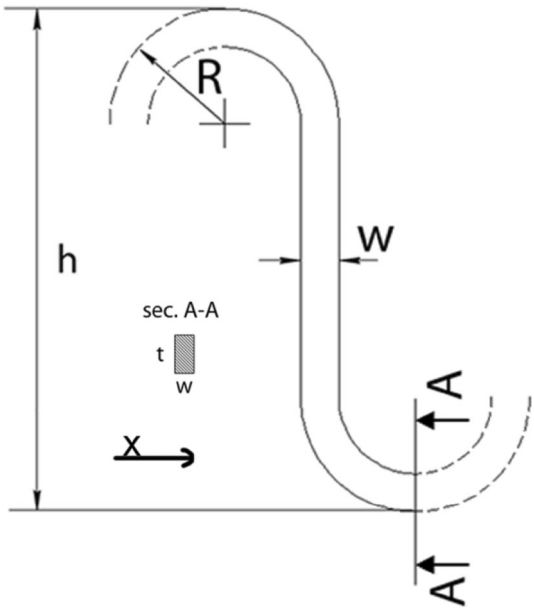

Fig. 1 Schematic of the elementary segment, at the basis of the SMA micro-element

Table 1 Final measured dimensions of the NiTi micro-elements

h, µm	*R*, µm	*w*, µm	*t*, µm
569 ± 8	95 ± 3	54 ± 9	90 ± 3

2.1 Material Preparation

A binary $Ni_{50.3}Ti_{49.7}$ (at.%) alloy was used for the realization of the SMA micro-elements. The alloy was produced by vacuum induction melting (VIM) in graphite crucible water cooled. The material was first hot forged and hot rolled at 950 °C and second cold rolled, with intermediate annealing treatments at 600 °C with following water quench, down to tapes of 120 µm in thickness with a final thickness reduction of 30%.

Finally, the NiTi tapes were thermal treated at 400 °C for 15 min in air, followed by water quench down to room temperature in order to promote the one way shape memory effect.

2.2 Geometry of the Micro-element

The micro-element geometry is composed by the replication of nine elementary segments, as the one depicted in Fig. 1. The shape of this segment can be identified by four geometrical parameters: the height *h*; the internal curvature radius *R*; the width *w*; and the thickness *t*, whose final dimensions are reported in Table 1. The NiTi micro-element was designed to produce linear motion along the *x*-axis direction (see Fig. 1).

2.3 Fabrication of the Micro-elements

The NiTi tapes were machined by means of a nanosecond fiber laser (model YLP-50 from IPG Photonics), generally used for micromachining (Ref 13). The laser system is completed with a LaserMech cutting head, having 60 mm focal lens and a coaxial nozzle (0.5 mm in diameter) for the adduction of the shielding gas, and an Aerotech 2D motion stage for the laser patterning. The main process parameters, used during the experiments, can be summarized in Table 2.

After the laser microcutting process, a chemical etching was undertaken in order to polish the sample surfaces from melted material and oxides, generated during the laser machining (Ref 14). The chemical etching, whose solution composition is 50% water, 40% HNO_3, and 10% HF, was performed for 7 min at room temperature inside ultrasonic cleaner to remove more efficiently the particles of the melted material (Ref 18). After

Table 2 Main process parameters used for the laser microcutting of the micro-elements geometry

Average power	50 W
Pulse frequency	80 kHz
Pulse duration	160 ns
Process speed	2 mm/s
Shielding gas/pressure	Argon @ 6 bar
Laser spot diameter	23 µm

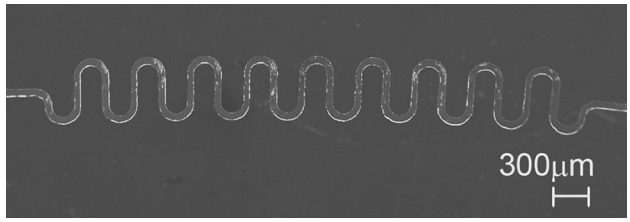

Fig. 2 SEM image of the final NiTi micro-element

Table 3 Sample denomination and brief description of the corresponding scope

Sample denomination	Sample description
Micro-element LC-P	Micro-element laser cut with *x*-axis (see Fig. 1) longitudinal to the rolling direction, followed by chemical etching
Micro-element LC-O	Micro-element laser cut with *x*-axis (see Fig. 1) transversal to the rolling direction, followed by chemical etching
Micro-element LC-P-T	Micro-element laser cut with *x*-axis (see Fig. 1) longitudinal to the rolling direction, followed by chemical etching, and subjected to an additional thermal treatment
Micro-element LC-O-T	Micro-element laser cut with *x*-axis (see Fig. 1) transversal to the rolling direction, followed by chemical etching, and subjected to an additional thermal treatment

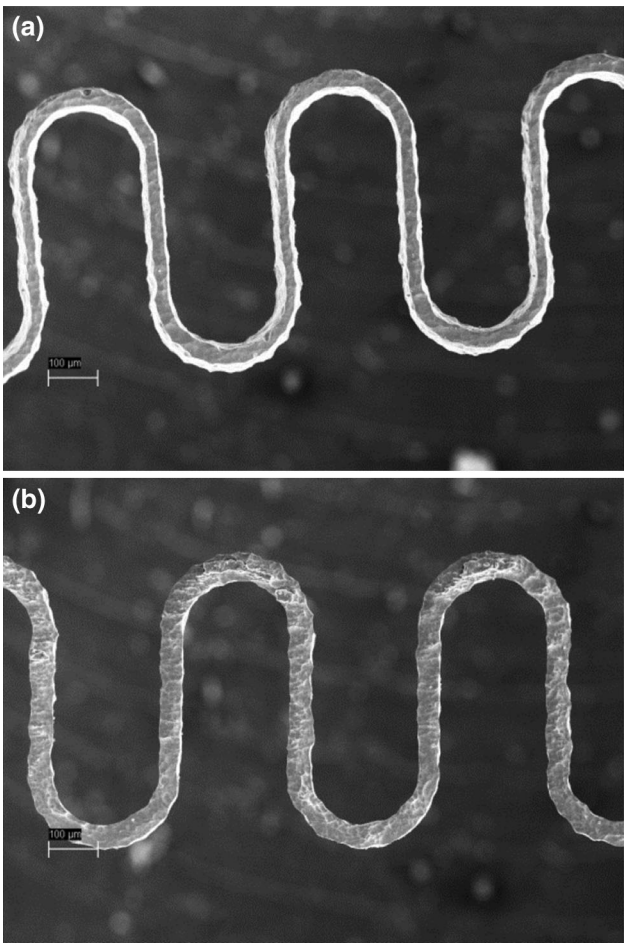

Fig. 3 SEM observations of the entrance (a) and exit (b) surfaces of a representative snake-like sample. The marker of the picture is 100 micron

the two fabrication steps, the final aspect of the micro-elements is shown in Fig. 2.

Different samples were fabricated to investigate the effect of the texture, due to the plastic deformation during the cold rolling, and the effect of an additional thermal treatment (at 450 °C for 15 min in air, then water quench down to room temperature), performed after the chemical etching.

The list of the samples, prepared for the functional characterization, as well as a small description of the aim of the single sample is reported in Table 3.

2.4 Characterization of the Micro-elements

Scanning electron microscope (SEM, model LEO 1430) was used to check the morphology of the sample surfaces after both laser microcutting and chemical etching. Calorimetric analysis has be proposed on small sample (few mg in mass) at the end of the fabrication for evaluating to characteristic temperatures and the transformation latent heats; for this purpose, a differential scanning calorimetric system (Q100 TA Instrum.), equipped with nitrogen cooling system, was adopted; complete thermal scan was done in a temperature range of (−100 to +100 °C) with a scanning rate of 10 °C/min. The identification of the finish characteristic temperatures was necessary for the functional characterization. For this purpose, thermo-mechanical tests were performed using a precise tensile testing machine (DMA—TA instrument mod. Q800), having a load cell of 18 N; strain recovery performances were evaluated during thermal cycling (five cycles) under different levels of constant load.

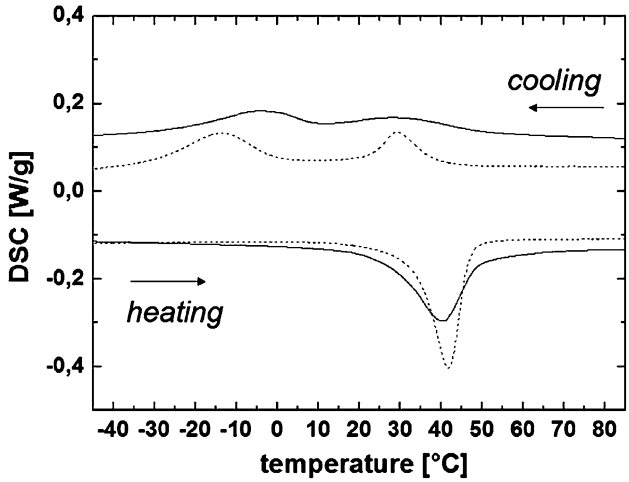

Fig. 4 DSC data of the SMA material before (straight line) and after (dotted line) the additional thermal treatment

3. Analysis of Results and Discussion

Figure 3 depicts the SEM images of a representative snake-like sample in its final state.

The effect of the additional thermal treatment (450 °C for 15 min) on the calorimetric response of the material is depicted in the DSC scan, reported in Fig. 4. The main effect of this additional treatment is a refinement of the peaks during both direct and reverse martensitic transformation. As a consequence, the temperatures of the peaks of the DSC signal do not strongly change, whilst the start transformation temperatures

Table 4 Characteristic temperatures of the no-treated and treated snake-like sample

	Rs, °C	Rp, °C	Rf, °C	Ms, °C	Mp, °C	Mf, °C	As, °C	Ap, °C	Af, °C
No-treated	54	28	14	19	−5	−40	26	40	51
Treated	40	30	22	0	−14	−40	33	42	47

Table 5 Transformation enthalpies during cooling and heating of the no-treated and treated snake-like samples

	ΔH cooling, J/g	ΔH heating, J/g
No-treated	−23	21
Treated	−20	18

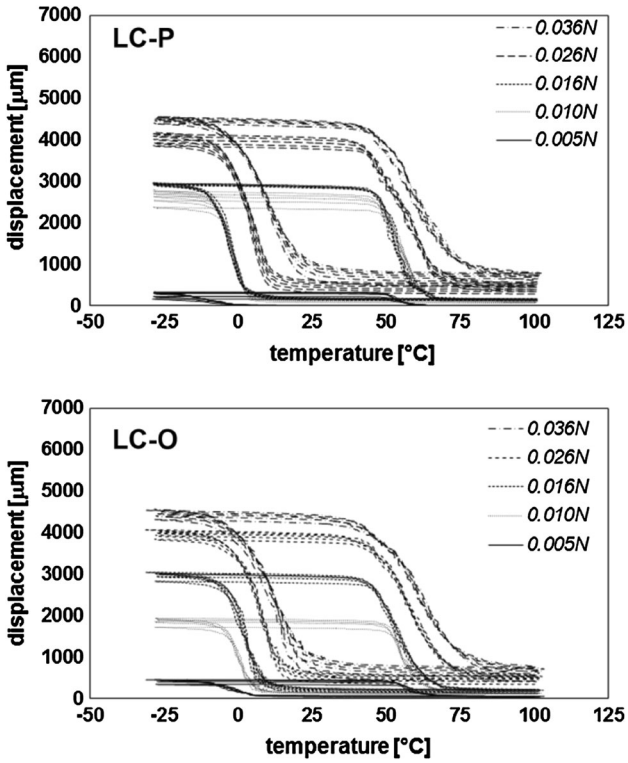

Fig. 5 Strain recovery curves, as function of temperature, of longitudinal and transversal samples at different applied loads

upon cooling and heating are decreased after the additional thermal treatment (see Table 4). Besides, in Table 5 a slight decreasing of the transformation entalpies is also visible.

Figure 5 depicts the strain recovery curves under different loads of the longitudinal and transversal samples. It can be noticed that the recovered strain is similar for the two samples. This behavior can be explained since the shape recovery under load has macroscopic effects with respect to the microscopic contributions of texture during this kind of tests. This means that the effect of the texture of the material, imposed by the previous cold rolling, does not cause any significant modifications on the strain recovery response. It can be explained through the stress distribution in the element geometry; in fact, the semi-circular part is characterized by the high stress values while the linear part does not, because the displacement is

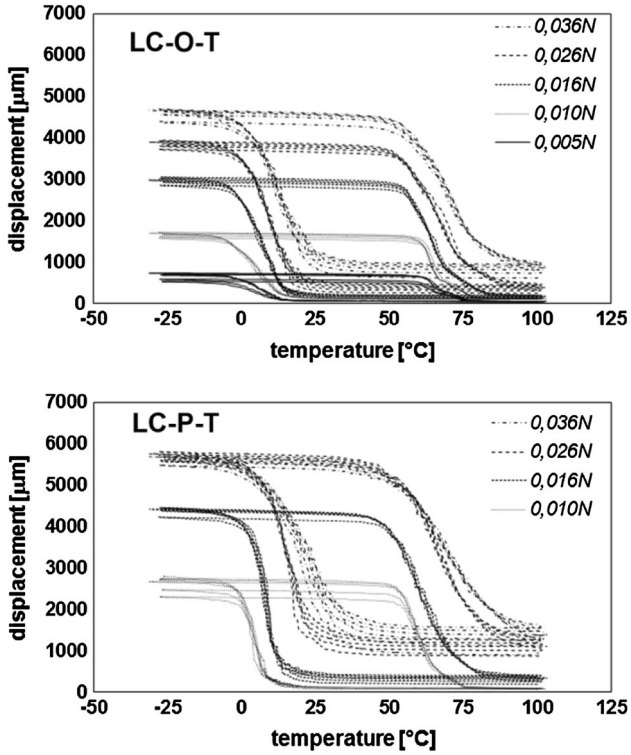

Fig. 6 Strain recovery curves, as function of temperature, of longitudinal and transversal thermal-treated samples at different applied loads

reached when the semi-arc is deformed along the load direction (see x-axis of Fig. 1).

Furthermore, it can be observed that in both cases the plastic deformation accumulated by the austenite and the martensite states increases with the increasing of the applied load. In particular, 0.016 N is the load limit above which the austenite starts to accumulate a marked permanent plastic deformation, not recoverable (see Fig. 5).

Figure 6 shows the shape recovery results of the snake-like samples, which underwent to the additional thermal treatment. It can be seen that the supplementary treatment leads to an overall improvement of the mechanical performances, even though it can be also noticed an increasing of the plastic deformation in both the martensite and the austenite phases. Additionally, the thermal treatment looks to put in evidence a modification of the stroke between the longitudinal and transversal samples. This could be explained for the lower stiffness, obtained after the thermal treatment, which makes these differences more visible. This effect needs to be more investigated on a larger number of samples for approaching a statistical analysis.

The additional thermal treatment effect on the mechanical performance of the snake-like sample is also visible on the

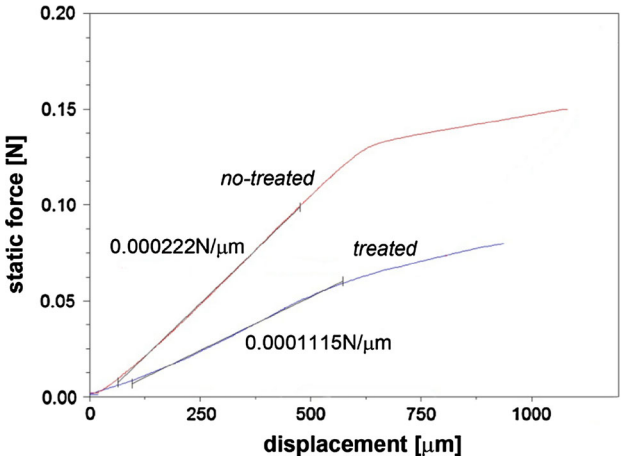

Fig. 7 Force vs. displacement curves of the treated and no-treated sample above the austenite finishing temperature

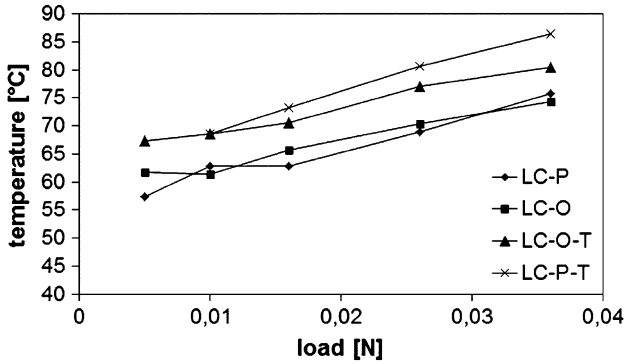

Fig. 8 Trend of the austenite finishing temperature Af, as function of the applied load, of the treated and no-treated sample

force versus displacement curve, reported in Fig. 7. Here, the response of the material above the austenite finishing temperature is reported. As it can be seen, the additional thermal treatment leads to a material more deformable, which is favorable for the performances of the actuator in terms of maximum available stroke. The change of slope, shown in Fig. 7, should be associated to both plastic deformation and stress-induced martensite. It is very hard to distinguish between the two contributes, because of the not elementary geometry of these micro-elements.

From the recovery tests of Fig. 5 and 6, it can be observed that the thermal hysteresis decreases with the increasing of the load. An overall increasing of the phase transformation temperatures is also visible. In Fig. 8, the trend of the austenite finishing temperatures of all samples as function of the applied load is plotted. It can be seen that the transition temperature Af increases with the applied load, as explained by the Clausius-Clapeyron relationship (Ref 19); besides, the additional thermal treatment also leads to an increasing of the transformation temperatures between the treated and the no-treated samples. The grain orientation does not seem to influence the Af temperature in the samples LC-P and LC-O while, according to the effect shown in Fig. 6, the samples thermally treated

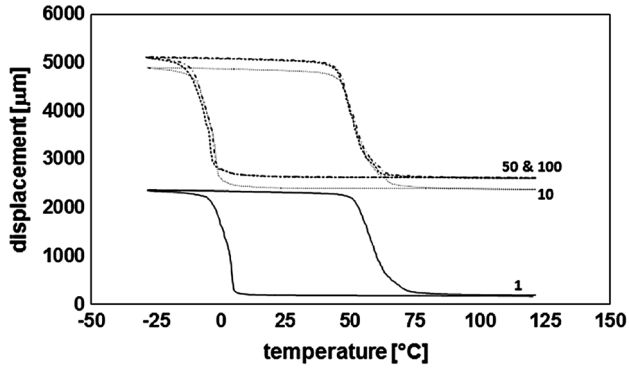

Fig. 9 Effect of the thermal cycling during the strain recovery tests of the LC-P sample under 0.016 N

(LC-P-T and LC-O-T) look to be influenced by their orientation with respect to the rolling direction.

Finally, recovery tests under a constant load of 0.016 N on the LC-P sample are shown in Fig. 9. The samples accumulate an elongation of about 2.5 mm of plastic deformation, from the initial length, in the austenite state within few tenths of thermal cycles. On the other side, the displacement remains stable and it can be set to about 2.5 mm. It can be also seen from Fig. 9 that the characteristic temperatures of the direct and reverse martensitic transformation are not significantly modified.

4. Conclusions

In this work, SMA micro-elements, able to be used as active elements for actuator applications, has been fabricated and their functional performances has been evaluated. Laser micromachining with subsequent surface chemical etching was adopted for the realization of these smart elements, having a so called snake-like geometry for guaranteeing relevant strokes. The following highlights can be summarized:

- The realized micro-elements are able to generate prospective values of the stroke, in the order of some millimeters (some tenths of % as axial deformation), under the application of loads equivalent to 10^3 times the element weight.
- The material texture does not seem to produce any significant variations of the strain recovery response. This could be explained for the stress distribution, according to the finite element method results; the semi-arc of the elements is the most stressed part of the geometry, having not a preferential direction in the case of circular geometry.
- A post-thermal treatment, after the fabrication of the micro-elements, seems to make more flexible the material for a longer displacement, if a load is applied. This should depend on the removal of the martensite domains, so a more deformable element can be obtained, according to different values of the Young modulus. Otherwise, no variation of the characteristic temperatures was detected.
- Finally, the evolution during thermal cycling under constant applied load was also checked. Both the relative and absolute strokes seemed to be characterized by a stabilizing effect by the 50th cycle.

References

1. H. Funakubo, *Shape Memory Alloys*, Gordon and Breach Science Publishers, New York, 1986
2. K. Otsuka and C.M. Wayman, *Shape Memory Materials*, Cambridge University Press, Cambridge, 1998
3. A. Nespoli, S. Besseghini, S. Pittaccio, E. Villa, and S. Viscuso, The High Potential of Shape Memory Alloys in Developing Miniature Mechanical Devices: A Review on Shape Memory Alloy Mini-actuators, *Sens. Actuators A*, 2010, **158**, p 149–160
4. C. Zanotti, P. Giuliani, A. Tuissi, S. Arnaboldi, and R. Casati, Response of NiTi SMA Wire Electrically Heated. *Proceedings of Esomat*, 2009, p 06037
5. Y. Bellouard, Shape Memory Alloys for Microsystems: A Review from a Material Research Perspective, *Mater. Sci. Eng. A*, 2008, **481–482**, p 582–589
6. T. Hsu, Miniaturization—A Paradigm Shift in Advanced Manufacturing and Education, *IEEE/ASME International conference on Advanced Manufacturing Technologies and Education in the 21st Century, Chia-Yi, Taiwan, Republic of China, August 10–15*, 2002
7. A.K. Dubey and V. Yadava, Laser Beam Machining—A Review, *Int. J. Mach. Tools Manuf.*, 2008, **48**, p 609–628
8. A. Nespoli, C.A. Biffi, R. Casati, E. Villa, A. Tuissi, and F. Passaretti, New Developments on Mini/Micro Shape Memory Actuators, *Smart Actuation and Sensing Systems—Recent Advances and Future Challenges*, G. Berselli, R. Vertechy, and G. Vassura, Ed., ISBN 978-953-51-0798-9
9. J. Meijer, G. Du, K. Hoffmann, O. Masuzawa, and S. Poprawe, Laser Machining by Short and Ultrashort Pulses, State of the Art and New Opportunities in the Age of the Photons, *CIRP. Ann. Manuf. Technol.*, 2002, **51**(2), p 531–550
10. B. Previtali, S. Arnaboldi, P. Bassani, C.A. Biffi, N. Lecis, A. Tuissi, M. Carnevale, and A. LoConte, Microcutting of NiTiCu Alloy with Pulsed Fiber Laser, ESDA2010-24943, *10th Biennial Conference on Engineering Systems Design and Analysis, Esda 2010, July 12–14, 2010, Istanbul, Turkey*, ISBN 978-0-7918-3877-8, Order No. I844CD
11. C.A. Biffi, P. Bassani, M. Carnevale, N. Lecis, A. Loconte, B. Previtali, and A. Tuissi, Effect of Laser Microcutting on Thermo-mechanical Properties of NiTiCu Shape Memory Alloy, *Met. Mater. Int.*, 2014, doi: 10.1007/s12540-013-6011-1
12. H. Zhao, J. Van Humbeck, and I. De Scheerder, Surface Conditioning of NiTi and Ta Stents, *Prog. Biomed. Res.*, 2001, **6**, p 439–448
13. A. Nespoli, C.A. Biffi, B. Previtali, E. Villa, and A. Tuissi, Laser and Surface Processes of NiTi Shape Memory Elements for Micro-actuation, *Metall. Mater. Trans. A.*, 2014, doi:10.1007/s11661-013-2177-x
14. C. A. Biffi, A. Nespoli, B. Previtali, A. Tuissi, NiTi Shape Memory Elements For Smart Micro-actuation: Laser Processing, Chemical Etching And Functional Characterization, *Proceedings of Eccomas, 6th ECCOMAS Conference on Smart Structures and Materials SMART2013*, 2013, online
15. A. Nespoli, E. Villa, and S. Besseghini, Thermo-mechanical Properties of Snake-Like NiTi Wires and Their Use in Miniature Devices, *J. Therm. Anal. Calorim.*, 2012, **109**, p 39–47
16. M. Kohl and K.D. Skrobanek, Linear Microactuators Based on the Shape Memory Effect, *Sens. Actuators A*, 1998, **70**, p 104–111
17. M. Kohl, B. Krevet, and E. Just, SMA Microgripper System, *Sens. Actuators A*, 2002, **97–98**, p 646–652
18. C.A. Biffi, L. Bonacina, A. Nespoli, B. Previtali, and A. Tuissi, Functional Characterization of NiTi Shape Memory Elements for Smart Micro-actuation, *Proceedings of the ASME 2013 Conference on Smart Materials, Adaptive Structures and Intelligent Systems, SMASIS2013, September 16–18, 2013, Snowbird, UT* (Order No: 1927CD)
19. P. Wollants, M. De Bonte, and J.R. Roos, A Thermodynamic Analysis of the Stress-Induced Martensitic Transformation in a Single Crystal, *Z. Metallk*, 1979, **70**(2), p 113–117